# FAILURE INVESTIGATION OF A HISTORIC TWO-SPAN UNREINFORCED MASONRY ARCH BRIDGE USING FINITE-ELEMENT ANALYSES

**Bryan P. Strohman[1] and Gunjeet Juneja[2]**
[1] Senior Staff II – Structures, Simpson Gumpertz & Heger Inc., 41 Seyon Street, Waltham, MA, 02453, USA, bpstrohman@sgh.com
[2] P.E. (CA), Malden, MA, gunjeetjuneja@gmail.com

## ABSTRACT
A failure investigation of a historic unreinforced masonry arch bridge with two 11.3 m (37 ft) span arches is presented. The unreinforced masonry arches were 7.0 m (23 ft) wide with a rise of 2.0 m (6.5 ft) and consisted of uniformly sized exterior granite arch-ring stones that were cut to precisely fit radially along the arch. The arches were bearing on granite skewback stones, which rested on unreinforced spread footings. The retrofit of the bridge envisioned two spans of reinforced concrete supported on two integral-abutment pile caps and one center pier with the two arches preserved for visual effect. During construction, large horizontal and vertical movements and cracks were observed. Finite-element analysis (FEA) models were created in PLAXIS and NASTRAN to assist in the structural failure investigation. The PLAXIS finite-element model evaluated the impact of the construction sequencing on the loading conditions and displacements of the bridge superstructure and surrounding soil. The NASTRAN model provided detailed response of the arches, including the development of cracks in the mortar that the PLAXIS model could not. An evaluation of the results from the PLAXIS and NASTRAN finite-element models and a comparison of these results to the structural damage observed are provided.

**KEYWORDS**: bridge, failure, investigation, FEA

## INTRODUCTION
Unreinforced masonry arch bridges have been constructed in the United States since the early nineteenth century. Due to deterioration and distress of these historic structures (often caused by age, weather, and increased applied live loads), many require retrofit or replacement to extend their service lives and maintain their cultural heritage. This paper describes the use of finite-element analyses to assist in the investigation of a historic unreinforced masonry arch bridge that failed during retrofit.

## BRIDGE DESCRIPTION
The bridge was constructed in 1909 and consisted of two 11.3 m (37 ft) span granite masonry arches. The unreinforced masonry arches were 7.0 m (23 ft) wide with a rise of 2.0 m (6.5 ft) and consisted of uniformly sized exterior granite arch-ring stones that were cut to precisely fit radially along the arch. The interior arch stones were cut more roughly and were of various sizes and shapes. The arches were bearing on granite skewback stones, which rested on unreinforced soil bearing spread footings. The exterior and interior arch-ring stones were set in mortar beds.

The spandrel walls above the arch were composed of irregularly-shaped uncoursed common rubble masonry stone set in mortar. Figure 1 shows an elevation of the north masonry arch post failure.

**Figure 1: North Masonry Arch with Rehabilitation Auxiliary Framing**

## FAILURE DURING CONSTRUCTION

The retrofit of the bridge envisioned a new two-span cast-in-place reinforced concrete bridge deck supported on two integral-abutment pile caps and one center pier cap constructed over and around and preserving the existing historic arches. Five steel H-piles were to support each pile cap and the reinforced concrete wingwalls and their footings were to be supported on two rows of steel H-piles, an interior row of vertical piles and an exterior row of battered piles.

Construction of the integral-abutment pile caps and center pier cap included (Table 2):

- Installation of soldier piles and lagging at each arch foundation.
- Excavation of the spandrel walls to the top of the granite thrust stones at the bridge foundations.
- Installation of struts between soldier piles.
- Installation of a concrete levelling pad in the excavation.
- Coring through the concrete levelling pad and bridge foundations.
- Backfilling of the core with peastone.
- Driving piles at the bridge foundations.
- Backfilling to the bottom of the new piles with peastone at the bridge foundations.
- Construction of pile caps and backfilling the excavation at the bridge foundations (removing struts as backfilling progressed).

The intent of the retrofit was for the arches to carry only the dead load, including their self-weight and the weight of the gravel fill between the top of the arches and the bottom of the new concrete slabs and pile caps, and the new structure would carry the remaining loads.

Following construction of the integral-abutment pile cap foundations for the new bridge, excavation to the bottom of the spread footings at the south and north spandrel walls was performed. Subsequently, during pile-driving for new wingwalls adjacent to the south abutment

foundation, the south masonry arch effectively failed and underwent large horizontal and vertical movements. Although the arch did not collapse, the arch-ring stones and spandrel walls were severely displaced from their original positions. The movements also caused significant lateral displacement of the top of the new south integral-abutment foundation. The north arch experienced deformation with large longitudinal cracks on the underside and minor displacement of its integral-abutment foundation. The failure also resulted in cracking of the spandrel walls at several locations. Figures 2 and 3 show the damage to the bridge's arches, spandrel walls, and rotation of the new foundations. The purpose of this paper is to present the use of finite-element modeling in assisting the failure investigation of the unreinforced masonry arch bridge.

**Figure 2: a) Failure of South Arch and Cracked Spandrel Wall; b) Rotation of New South Abutment**

**Figure 3: a) Opening in Mortar Joints between Exterior Ring Stones; b) Gap between Bottom of Northeast Spandrel Wall and Top of North Abutment**

## INVESTIGATIVE FINITE-ELEMENT MODELS

Two finite-element analysis models were created to assist in the structural failure investigation: a simplified two-dimensional (2D) plane strain finite-element model of the surrounding and supporting soil strata, spread footings, arches, and spandrel walls in PLAXIS V9.02 (PLAXIS),

and a more complex 2D finite-element model of the exterior granite blocks of the arches using NASTRAN. PLAXIS and NASTRAN are general-purpose finite-element analysis (FEA) software packages. The FEA models were used to compute the structural response of the bridge and to compare it to the arch and foundation structural damage observed during a post-failure inspection. The results of the finite-element analyses were also used to evaluate the risk and contribution to the arch-bridge abutment foundation sliding and/or a soil-bearing capacity failure during retrofit construction. A brief commentary on the potential for vibrations-induced ground settlements is provided.

## PLAXIS MODEL

The purpose of the PLAXIS model was to determine the impact of the construction sequencing on the loading conditions and displacements of the arches, and to obtain horizontal and vertical spring coefficients to represent the foundation stiffness in the structural model of the arches created in NASTRAN.

The 2D PLAXIS model included the following features:

- Due to the lack of detailed soil data to develop soil modeling parameters, all materials including soil and stone, with the exception of the bridge spandrel wall material, were modeled as linear elastic. The bridge spandrel wall material was modeled as a Mohr-Coulomb soil. Table 1 summarizes the soil and structure material properties used in the PLAXIS model and Figure 4 shows an overall view of the PLAXIS model with material definitions

- Dewatering occurred where the excavation extended below the groundwater elevation. The groundwater elevation was considered at the same level as the bottom of the excavation during dewatering.

**Table 1: Material Properties Used in 2D PLAXIS Model**

| Material | Unit Weight, $kN/m^3$ (pcf) | Poisson's Ratio | Young's Modulus (E), MPa (ksi) |
|---|---|---|---|
| Granite | 26.7 (170) | 0.2 | 68,947.6 (10,000) |
| Sand Fill | 18.9 (120) | 0.3 | 33.1 (4.8) |
| Medium-Dense Sand | 18.9 (120) | 0.3 | 41.4 (6.0) |
| Medium-Dense to Dense Sand w/ Cobbles | 22.0 (140) | 0.3 | 63.4 (9.2) |
| Peastone | 21.2 (135) | 0.3 | 27.6 (4.0) |
| Uncompacted Gravel | 20.4 (130) | 0.2 | 95.8 (13.9) |
| South Abutment Footing (boulder foundation) | 23.6 (150) | 0.2 | 689.5 (100) |
| Center Pier and North Abutment Footing | 23.6 (150) | 0.17 | 27,792.8 (4,031) |
| Spandrel Walls (Mohr-Coulomb) | 25.9 (165) | 0.2 | 68.9 (10) |
| | Cohesion = 3.4 kPa (0.5 psi), Friction angle = 40° | | |

Table 2 summarizes the construction sequence modeled in PLAXIS. Figures 5 to 7 show a graphical representation of the PLAXIS model at Steps 4, 11, and 16; Step 16 is the final sequence step when failure occurred.

**Table 2: Construction Sequence Included in 2D PLAXIS Model Staged Analysis**

| Step No. | Description |
|---|---|
| 0 | Virgin site prior to bridge construction. |
| 1 | Excavate soil to river mud line. Activate arch and arch foundations only, for verification of arch self-weight. |
| 2 | Activate spandrel walls. |
| 3 | Activate soldier piles (Displacements set to zero after Step 2). Soldier piles and lagging modeled as earth support at the ends of the spandrel walls. |
| 4 | Excavate spandrel walls to top of granite thrust stones at bridge foundations. Activate struts. Struts modeled between soldier piles to hold open the spandrel wall excavation (Figure 5). |
| 5 | Activate concrete leveling pad in excavation at bridge foundations. |
| 6 | Core through concrete leveling pad and arch foundations. Backfill core with peastone. Activate driven piles at bridge foundations. Deactivate lower strut in excavation. |
| 7 | Backfill to bottom of new pile cap with peastone at bridge foundations. |
| 8 | Install pile caps and backfill to top of excavation with peastone at bridge foundations. Deactivate upper strut. Partial removal of soldier piles. |
| 9 | Excavation at south spandrel wall to the bottom of granite skewback stone. |
| 10 | Excavation at south spandrel wall to the bottom of footing. |
| 11 | Over-excavation at south spandrel wall 4 ft below the bottom of footing (Figure 6). |
| 12 | Backfill over-excavation with uncompacted gravel to the bottom of footing. |
| 13 | Excavation at north spandrel wall to the bottom of granite skewback stone. |
| 14 | Excavation at north spandrel wall to the bottom of footing. |
| 15 | Over-excavation at north spandrel wall 2 ft below the bottom of footing. |
| 16 | Install three driven wingwall foundation piles adjacent to south bridge foundation (Figure 7). |

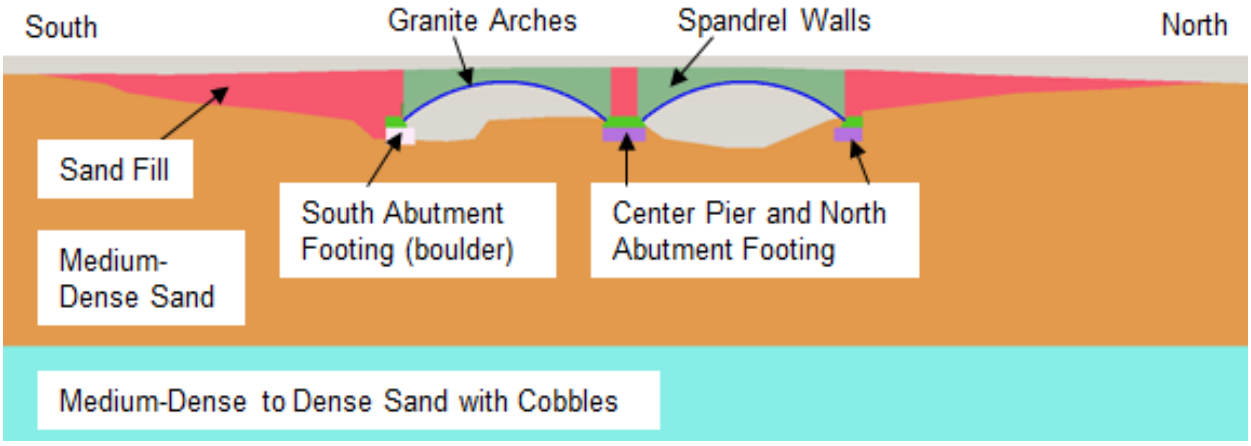


**Figure 4: Overall View of PLAXIS Model**

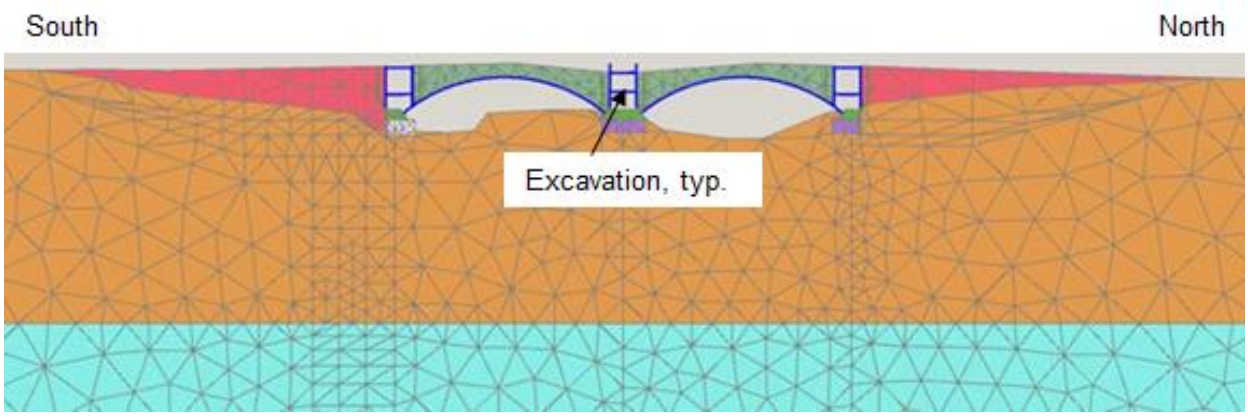


**Figure 5: Step 4 – After Excavation of Spandrel Walls to Top of Granite Thrust Stones at Bridge Foundations (Excavation Supported by Soldier Piles)**

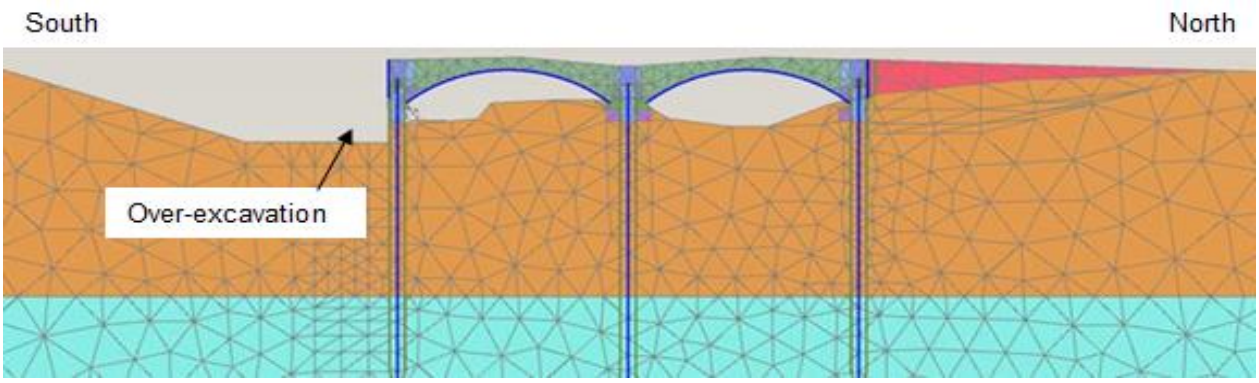


**Figure 6: Step 11 – After Over-Excavation at South Spandrel Wall 4 ft Below the Bottom of Footing**

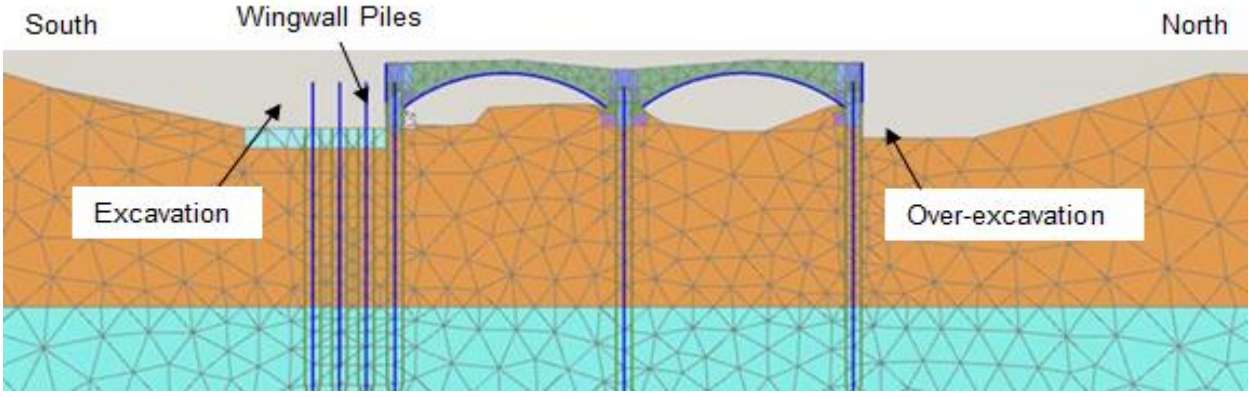


**Figure 7: Step 16 – After Driving of New South Abutment Wingwall Foundation Piles**

## NASTRAN MODEL

The purpose of the NASTRAN model was to evaluate the stability of the bridge based on a 0.76 m (2.5 ft) thick longitudinal slice of the bridge. The arches were modeled using 0.76 m (2.5 ft) thick plate elements representing each arch, which consisted of twenty-seven stones mortared together. The plate elements were connected together with interface (gap) elements that can transmit compression and shear forces from one stone to the neighboring stone. The interface element also allowed separation of one corner of the plate element from its neighbor. The plate elements were modeled with a granite elastic modulus of 68,947.6 MPa (10,000 ksi), a Poisson's ratio of 0.2, and a density of 26.7 kN/m$^3$ (170 pcf).

Linear spring elements with spring constants based on the results from the PLAXIS analysis for Step 2 and Step 16 were used for modeling the footing behavior in NASTRAN. Figure 8 shows the 2D NASTRAN finite-element model that includes the south and north arches and connecting skewback stones over the center footing.

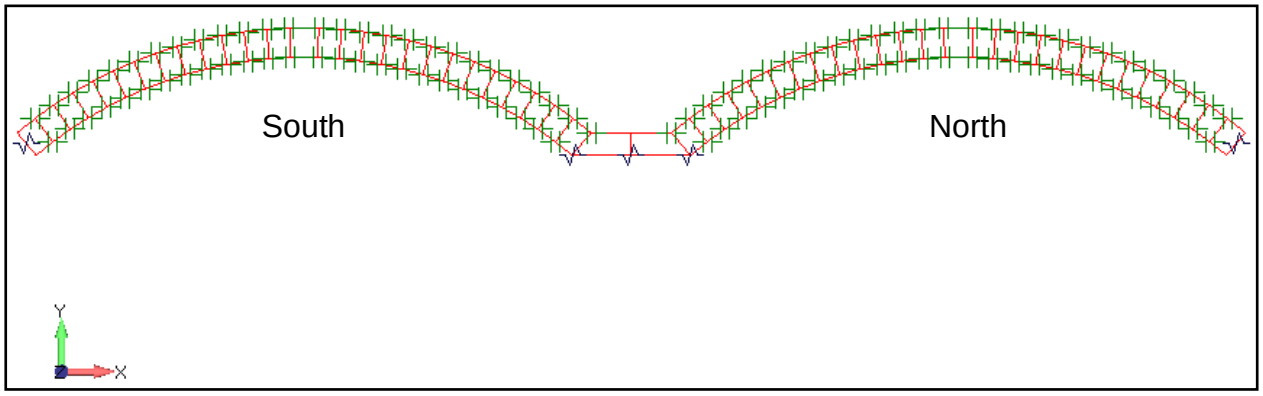


**Figure 8: 2D NASTRAN FEA Model**

The loading of this model is the weight of the granite arch itself and the weight of the stone spandrel walls (density of 25.9 kN/m$^3$ (165 pcf)) acting on the arches and the center pier. Nonlinear elastic analyses were performed of the arches for these loads with the PLAXIS Step 2 and Step 16 foundation spring constants.

## EVALUATION OF THE PLAXIS FINITE-ELEMENT ANALYSIS

The PLAXIS finite-element model provides a detailed representation of the effects of soil-structure interaction and of the construction sequence utilized prior to failure. These features allow PLAXIS to provide accurate overall results for forces acting on the arch foundations and the soil below these foundations. However, in PLAXIS the arch structures are modeled very simply, and the bending strength of the arches is overestimated because the effects of arch hinging (due to partial separation of stones) are not captured.

Table 3 summarizes the loading and deformation conditions obtained from the PLAXIS model output and the calculated equivalent horizontal and vertical soil spring values at each abutment and the center pier for Step 2 (prior to retrofit construction) and Step 16 (last step prior to failure). Spring stiffnesses were calculated considering an effective width of 0.76 m (2.5 ft), to match the geometry of the NASTRAN model. The vertical forces derived from PLAXIS for

Step 1 were compared to hand calculations of the behavior of the arch model for verification and showed good agreement.

**Table 3: Results of 2D PLAXIS Model**

| Step No. | Thrust, kN/m (plf) (1) | Shear, kN/m (plf) (2) | Horizontal Movement, mm (in.) (3) | Vertical Movement, mm (in.) (3) | Horizontal Force, kN/m (plf) (4) | Vertical Force, kN/m (plf) (5) | Horizontal Stiffness, kN/mm (pli) (6) | Vertical Stiffness, kN/mm (pli) (6) |
|---|---|---|---|---|---|---|---|---|
| South-Abutment Foundation | | | | | | | | |
| 2 | -273 (-18,710) | -193 (-13,200) | -4.6 (-0.179) | -9.1 (-0.359) | -85 (-5,848) | -323 (-22,138) | 14 (8.2E+4) | 26 (1.5E+5) |
| 13 | -376 (-25,749) | -213 (-14,597) | | | | | | |
| 16 | -346 (-23,742) | -158 (-10,852) | -4.6 (-0.179) | -7.7 (-0.304) | -164 (-11,212) | -344 (-23,574) | 28 (1.6E+5) | 33 (1.9E+5) |
| Center Pier – South End | | | | | | | | |
| 2 | -286 (-19,598) | 137 (9,403) | 0.5 (0.020) | -9.2 (-0.364) | -131 (-8,969) | -289 (-19,800) | 193 (1.1E+6) | 25 (1.4E+5) |
| 16 | -163 (-11,171) | 211 (14,485) | -2.7 (-0.106) | -4.6 (-0.179) | 11 (753) | -267 (-18,277) | 3 (1.8E+4) | 44 (2.5E+5) |
| Center Pier – North End | | | | | | | | |
| 2 | -265 (-18,156) | -177 (-12,124) | 0.5 (0.020) | -9.8 (-0.384) | -89 (-6,115) | -306 (-20,958) | 135 (7.7E+5) | 25 (1.4E+5) |
| 16 | -166 (-11,346) | -225 (-15,450) | -2.5 (-0.099) | -3.6 (-0.140) | 18 (1,240) | -279 (-19,128) | 5 (3.1E+4) | 60 (3.4E+5) |
| North-Abutment Foundation | | | | | | | | |
| 2 | -270 (-18,516) | 179 (12,267) | 5.8 (0.228) | -5.5 (-0.218) | -92 (-6,299) | -311 (-21,299) | 12 (6.9E+4) | 42 (2.4E+5) |
| 16 | -328 (-22,484) | 123 (8,456) | -1.3 (-0.052) | -0.8 (-0.033) | -172 (-11,788) | -305 (-20,930) | 100 (5.7E+5) | 280 (1.6E+6) |

(1) Negative thrust force indicates compression.
(2) Negative shear acts outwards and upwards.
(3) Negative displacement acts vertically downward and laterally to the south.
(4) Negative horizontal force acts to the south.
(5) Negative vertical force is downward.
(6) Spring stiffnesses were calculated considering an effective width of 0.76 m (2.5 ft), to match the NASTRAN model.

The soil stiffness values (i.e., Young's modulus, E) included in the PLAXIS model represents the best estimate. To evaluate potential changes in analysis results due to stiffness values other than those considered in the initial model, three separate sensitivity analyses were performed in which the elastic modulus € values of (1) the granite arch and foundation stones, (2) boulder foundation, and (3) foundation soil, was reduced by half. These sensitivity analyses indicate that lowering the stiffness values of these materials has no significant impact on the value of the vertical loads, and the vertical and horizontal displacements calculated. However, lower stiffness values for the granite and boulder foundations, and for the foundation soil, resulted in 30 – 80% reductions in the value of horizontal reaction forces.

## EVALUATION OF THE NASTRAN FINITE-ELEMENT ANALYSIS

The NASTRAN finite-element model provides a representation of the arch structure, including direct modeling of the separation of portions of contact areas of individual stones from their

adjacent neighbors. However, in NASTRAN, the soil is not included in the structural model, except as the spring constants for the supports (taken from PLAXIS results). Hence, all soil characteristics are represented in the NASTRAN model as soil springs resulting in horizontal arch-support reactions that are likely conservative (on the high side).

Figure 9 shows the deformed shape of the arch for Step 2 spring stiffness values with the contours representing the forces (compression shown positive) transmitted by the interface elements. The analysis with Step 2 footing spring stiffness values indicates that in both arches gaps open at the corners of the granite blocks located near the crown and the center pier. These gaps reflect that the arch behavior tends towards a three-hinged arch condition under Step 2 conditions and foundation spring stiffness values. The analysis with Step 16 conditions and foundation spring stiffnesses also results in a hinge near the crown for the two arches with another hinge near the center pier in the north arch. A hinge does not form in the south arch near the center pier at this step until the vertical support of the abutment of the south arch settles vertically by approximately 19 mm (0.75 in.).

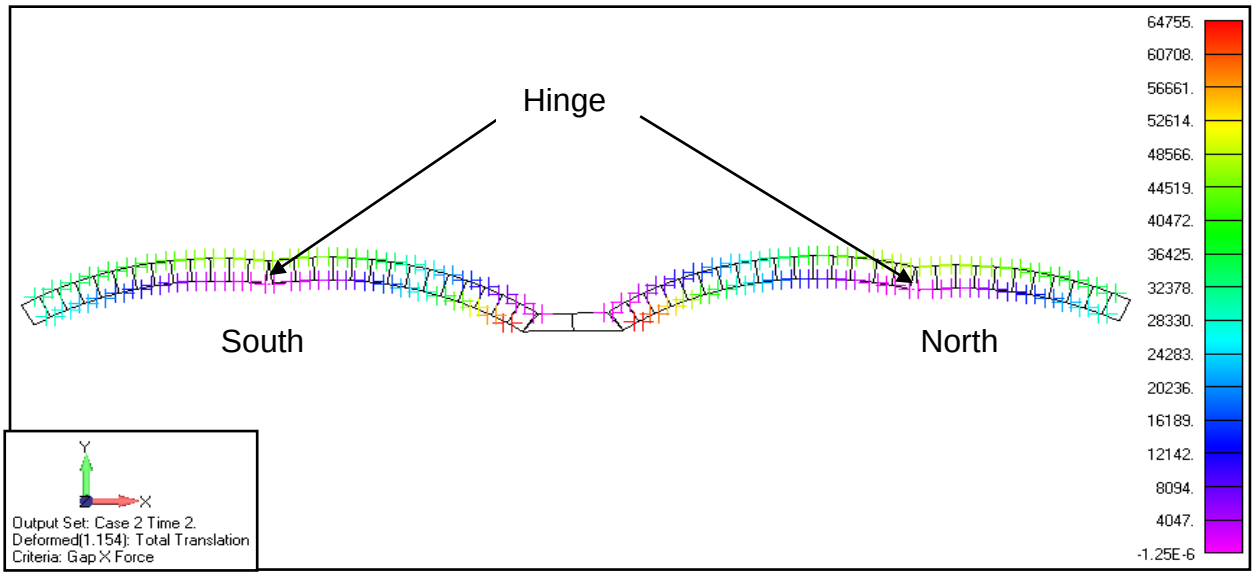


**Figure 9: Arch Gap Forces with Deformed Shape (x50) under Self Weight and Rubble Spandrel Wall Weight with PLAXIS Step 2 Footing Spring Stiffness Values**

## COMPARISON OF FINITE-ELEMENT ANALYSIS RESULTS TO STRUCTURAL DAMAGE

The damage observed during a post failure inspection indicated that the south masonry arch span experienced large movements in the range of about 1 ft (including movement of its foundations, arch-ring stones, and spandrel walls) horizontally and vertically. The observed condition of the south arch is similar to that of a three-hinged arch. As shown in Figure 9, the NASTRAN finite-element model results depict less vertical settlement but localized hinging at about the same locations observed during the post failure inspection.

Elementary structural theory indicates that a three-hinged arch is statically determinate and that the internal forces of statically determinate structures are not affected by support settlement. The

results of our NASTRAN model analyses demonstrated that vertical settlement of the south abutment beyond 19 mm (0.75 in.) results in no change in gap forces in the south arch; these gap forces represent the thrust in the arch. The combined results of our analyses indicate that support settlements exceeding 19 mm (0.75 in.) were likely to occur during the construction process; possibly due to arch-foundation sliding and/or a soil-bearing capacity failure during pile-driving for new wingwalls following installation of the retrofit integral-abutment pile foundations.

Use of the finite-element analysis results to assist in the evaluation of the risk and contribution of arch-foundation sliding or soil-bearing capacity failure indicated that during Step 16, upon removal of the soil above and adjacent to the arch abutment foundations, as required for construction of the new foundations, the static factors of safety against sliding of the granite arch abutment and boulder foundation reduced to slightly less than 1.0. Similarly, the static factor of safety against bearing failure of the arch abutment foundations reduced significantly, from values greater than 40 prior to Step 16 to values slightly less than 1.0. The extremely low calculated factors of safety indicate that the arch-bridge-foundation system was only marginally stable during Step 16, and that any subsequent disturbance, such as pile-driving vibrations could induce rapid transient vertical and horizontal translations, resulting in cumulative movement and potential failure of the structure.

After failure, the bridge necessitated demolition and replacement with precast concrete arch elements.

## SUMMARY AND CONCLUSIONS

Design of retrofit concepts for historic masonry structures often requires forethought on all possible conditions that the existing site and structural system will be subjected to during retrofit construction. This includes the challenge of maintaining continuity of load path, which requires thorough analysis to assess the associated risk. We presented a case study on a failure investigation of a historic two-span unreinforced masonry arch bridge on soil-bearing foundations. Our investigative effort included finite-element analyses using general-purpose FEA software packages PLAXIS and NASTRAN to examine the structure-soil-foundation system. Good comparison between the analysis results and the observed damage in the case study presented above demonstrates that the finite-element method of analysis using general-purpose FEA software packages, if used appropriately, can be a powerful tool for evaluating masonry structural systems.